Extended Flight Bouts Require Disinhibition from GABAergic Mushroom Body Neurons

Steffy B Manjila, Maria Kuruvilla, Jean-François Ferveur, Sanjay P Sane, Gaiti Hasan

Article

Current Biology

Extended Flight Bouts Require Disinhibition from GABAergic Mushroom Body Neurons

Graphical Abstract

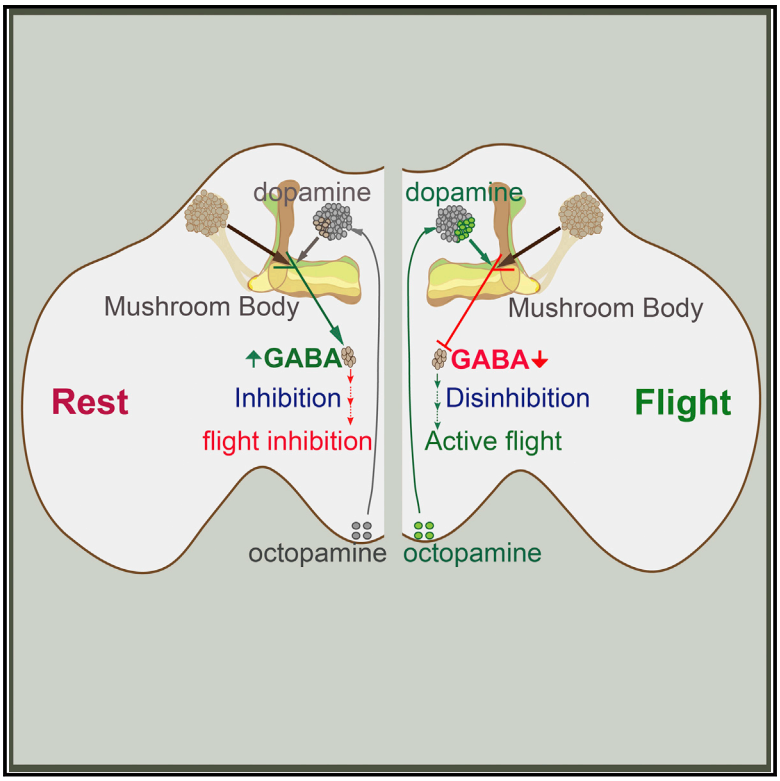

Authors

Steffy B. Manjila, Maria Kuruvilla, Jean-Francois Ferveur, Sanjay P. Sane, Gaiti Hasan

Correspondence

gaiti@ncbs.res.in

In Brief

Manjila et al. demonstrate a neuronal pathway required to maintain extended flight bouts in *Drosophila*. Octopaminergic inputs to specific dopaminergic neurons inhibit GABAergic mushroom body output neurons to maintain this "flight state," which probably helps the fly find food sources, suitable egg-laying sites, or mates in its natural environment.

Highlights

- PAM dopaminergic neurons are active during flight and require octopaminergic inputs
- Flight-regulating PAM neurons project to the β'1 lobe of the mushroom body
- Shorter flight bouts are observed upon activation of GABAergic β'1 output neurons
- PAM neurons inhibit GABAergic β'1 output neurons to support extended flight bouts

Manjila et al., 2019, Current Biology *29*, 1–11
January 21, 2019
https://doi.org/10.1016/j.cub.2018.11.070

CellPress

Please cite this article in press as: Manjila et al., Extended Flight Bouts Require Disinhibition from GABAergic Mushroom Body Neurons, Current Biology (2018), https://doi.org/10.1016/j.cub.2018.11.070

Current Biology
Article

CellPress

Extended Flight Bouts Require Disinhibition from GABAergic Mushroom Body Neurons

Steffy B. Manjila,[1] Maria Kuruvilla,[1] Jean-Francois Ferveur,[2] Sanjay P. Sane,[1] and Gaiti Hasan[1,3,*]
[1]National Centre for Biological Sciences, Tata Institute of Fundamental Research, Bangalore 560065, India
[2]Centre des Sciences du Goût et de l'Alimentation, UMR6265 CNRS, UMR1324 INRA, Université de Bourgogne Franche-Comté, Dijon, France
[3]Lead Contact
*Correspondence: gaiti@ncbs.res.in
https://doi.org/10.1016/j.cub.2018.11.070

SUMMARY

Insect flight is a complex behavior that requires the integration of multiple sensory inputs with flight motor output. Although previous genetic studies identified central brain monoaminergic neurons that modulate *Drosophila* flight, neuro-modulatory circuits underlying sustained flight bouts remain unexplored. Certain classes of dopaminergic and octopaminergic neurons that project to the mushroom body, a higher integrating center in the insect brain, are known to modify neuronal output based on contextual cues and thereby organismal behavior. This study focuses on how monoaminergic modulation of mushroom body GABAergic output neurons (MBONs) regulates the duration of flight bouts. Octopaminergic neurons in the sub-esophageal zone stimulate central dopaminergic neurons (protocerebral anterior medial, PAM) that project to GABAergic MBONs. Either inhibition of octopaminergic and dopaminergic neurons or activation of GABAergic MBONs reduces the duration of flight bouts. Moreover, activity in the PAM neurons inhibits the GABAergic MBONs. Our data suggest that disinhibition of the identified neural circuit very likely occurs after flight initiation and is required to maintain the "flight state" when searching for distant sites, possibly related to food sources, mating partners, or a suitable egg-laying site.

INTRODUCTION

The evolution of flight enhanced the ability of insects to evade predators, search for food or egg-laying sites, and escape from unfavorable environmental conditions or predators. The path and duration of insect flight is determined by the integration of multiple sensory inputs and their coordination with the flight motor circuit. Such integration occurs in discrete but connected centers of the insect central brain [1, 2]. For instance, the insect central complex (CC) plays an important role in integrating information about heading direction and angular orientation of flight [2] upon motion detection in the optic medulla [3], and different regions of the CC, such as the fan-shaped body (FB), process visual information during flight [4]. In addition to the CC, flight is also modulated by antennal mechanosensory neurons located in the AMMC (antennal mechanosensory and motor center), that receive inputs from Johnston's organs and regulate wing motor reflexes during flight [1, 5]. In honeybees, the mushroom bodies also regulate flight [6, 7].

We have reported previously that flight bout durations are reduced when Frizzled2 (Fz2)-mediated calcium signaling is impaired in the central protocerebral anterior medial (PAM) dopaminergic neurons (DANs) during pupal stages of *Drosophila* development [8]. The function of PAM-DANs has primarily been investigated in the context of olfactory learning and memory, where they send reward as well as aversive signals, based on appropriate olfactory cues to synapses in the mushroom bodies (MBs)—another higher brain center [9–11]. Recent studies have demonstrated that MBs also integrate the animal's internal state with extrinsic cues to modulate behavior [12]. Integration of extrinsic and intrinsic cues by the MB is done in the neuropil regions formed by projections from MB intrinsic neurons or the Kenyon cells (KCs). MBs are lobed structures consisting of vertical (α and α') and horizontal lobes (β, β', and γ), which are further innervated by pre-synaptic terminals of PAM-DANs and protocerebral posterior lateral 1 (PPL1) clusters [13, 14] and dendrites of MB output neurons (MBONs). The DANs induce heterosynaptic plasticity at the KC-MBON synapses [12]. PAM-DAN activity can thus modulate synaptic outputs of specific MB lobes. Based on the existing role of octopamine (OA) in insect flight [15, 16], we hypothesized that, in the context of flight too, PAM-DAN activity may be modulated by OA. OA is analogous to vertebrate norepinephrine, and in de-afferented locust and moth preparations, it very effectively evoked fictive flight [17, 18]. Moreover, genetic disruption of octopaminergic neurons in *Drosophila* reduces the duration of flight bouts [15], and a class of G-protein-coupled receptors (GPCRs) for OA, referred to as Oamb (octopamine receptors in mushroom bodies) are strongly expressed on PAM neurons [19]. The Oamb has so far been implicated in sleep and metabolism [20], aggression [21], regulation of sugar consumption [22], and ovulation [23].

Here, we show that octopaminergic inputs, including neurons from the sub-esophageal zone (SEZ), activate PAM β'1 neurons, which inhibit MBON-β'1 to maintain longer flight bouts. Our findings support a model where GABAergic outputs from MBON-β'1 help maintain the fly at rest. For longer flight bouts, such

inhibitory outputs from the MB require negative modulation by dopamine, probably during acute flight.

RESULTS

Sustained Flight Requires an OA Receptor on Adult Dopaminergic PAM Neurons

To investigate whether central PAM-DANs function during adult flight, a recently developed genetic tool referred to as CaMPARI (calcium-modulated photoactivatable ratiometric integrator) was employed, where an irreversible conversion of green to red fluorescent protein occurs when there is coincidence of experimenter-controlled UV light exposure with neuronal activity [24]. Flies expressing CaMPARI in PAM-DANs using the *R58E02-GAL4* [10] strain (henceforth referred to as *PAM-DANs GAL4*; see Table S1) were exposed to UV light during air-puff-stimulated flight. As controls, flies of the same genotype were exposed to UV without an air puff stimulus. Green to red fluorescence shifts were observed in a subset of PAM neurons from dissected brain samples, when UV exposure was coupled with air-puff-stimulated flight (Figures 1A and 1B). Red to green fluorescence ratios were significantly higher in flies with UV exposure as compared to UV exposure of non-stimulated static flies (Figure 1C), indicating the presence of neuronal activity in some PAM neurons during tethered flight.

Previous studies have identified OA as a modulator of insect flight duration [15, 16], and it is well established that PAM neurons receive octopaminergic inputs [9, 19]. Therefore, we tested flight bout durations after knockdown of octopaminergic receptors on PAM neurons. Significant deficits in flight bout durations were observed by knockdown of *Oamb* and *Octβ1* receptor with the *PAM-DANs GAL4* strain (Figures 1D and S1A). Specificity of *Oamb* and *Oct β1* knockdown was confirmed by knockdown with two or more independent RNAi strains (Figure S1A). Moreover, flight deficits were also observed in $Oamb^{584}$, an Oamb-null mutant [25] (Figure 1D), that were rescued to a modest extent by overexpressing a transgene encoding Oamb in PAM neurons (Figure S1B). Knockdown of the remaining OA receptors in PAM neurons did not elicit significant flight deficits (Figure S1A). Subsequent analyses focused on Oamb, the expression of which is well documented in PAM neurons [19]. Deficits in flight bout durations by *Oamb* knockdown in PAM-DANs were reconfirmed with an independent strain, *R76F05-GAL4* [26] (Figure 1D; Table S1).

To test the requirement of Oamb for acute flight, *Oamb* knockdown in PAM neurons was limited to specific developmental stages by the TARGET (temporal and regional gene expression targeting) system where simultaneous expression of a $GAL80^{ts}$ transgene allows RNAi expression at 29°C, but not at 18°C [27]. Flight bouts were reduced significantly upon *Oamb* knockdown in PAM neurons of adults (~200 s) as compared to controls (~500 s; Figure 1E). Flies with larval and pupal knockdown of *Oamb* displayed normal flight bouts (Figure S1C). Expression of a hyperpolarizing potassium channel Kir2.1 [28] in adult PAM neurons also resulted in a significant reduction of flight bout durations, confirming that activity in PAM neurons supports longer flight durations (Figures 1F and S1D). Neither expression of Kir2.1 nor *Oamb* knockdown resulted in a decrease of PAM-DAN cell numbers (Figures S1E and S1F).

OA Neuron Activity Is Required for Adult Flight and Stimulates PAM-DANs

The adult requirement of Oamb suggests that flight bout durations are modulated by octopaminergic inputs to the PAM-DANs. Previous studies have demonstrated that genetic ablation of octopaminergic neurons reduces flight [15]. However, such flight deficits could also have arisen from octopaminergic modulation of flight circuit development. Therefore, a requirement for OA neuron activity during adult flight needed testing. For this purpose, a temperature-sensitive mutant of the dynamin ortholog, Shibire^{ts} (Shi^{ts}), was expressed in octopaminergic neurons marked by *Tdc2-GAL4* (henceforth referred to as *OA-GAL4*) [29]. The Shi^{ts} transgene inactivates at 30°C, leading to a block in synaptic vesicle recycling and thus synaptic function [30]. Expression of Shi^{ts} in adult octopaminergic neurons followed by a shift to the non-permissive temperature of 30°C significantly reduced flight bout durations in OA>Shi^{ts} (~250 s) as compared to controls (~500 s; Figure 2A). A significant decrease in maintenance of longer flight bouts was also observed by adult-specific inactivation of OA neurons with *Kir2.1* expressed using the TARGET system (Figure 2B). Next, we expressed Shi^{ts} in octopaminergic neuronal subsets using available GAL4 drivers that mark among others the ventral paired medial 4 (OA-VPM4) neurons (see Table S1) [9, 13]. Inactivation of synaptic vesicle recycling in neurons marked by *MB113C-GAL4* (marks VPM4 neurons exclusively, henceforth referred to as *VPM4-GAL4*) resulted in flight deficits comparable to those observed with other subset GAL4s, which mark neurons other than VPM4 (Figure 2A). Thus, the OA-VPM4 neurons are required for maintenance of longer flight bouts. However, inputs from other octopaminergic neurons to the PAM cluster are also very likely required, because significantly greater flight deficits were observed in *OA-GAL4*>Shi^{ts} flies as compared to *VPM4-GAL4*>Shi^{ts} flies. Moreover, optogenetic activation of octopaminergic neurons in *ex vivo* brain preparations by expression of a red shifted channelrhodopsin, *CsChrimson* (*UASChrimson*) [31] evoked strong calcium transients in PAM neurons (*PAM-DANs LexA*>*LexAopGCaMP6f*; Figures 2C–2E). Calcium transients were also elicited in PAM neurons by activation of OA-VPM4 neurons (*VPM4-GAL4*). However, these signals were weaker as compared to activation of entire octopaminergic neurons (*OA-GAL4*>*UASChrimson*; Figures 2C–2E). Therefore, PAM neurons receive octopaminergic inputs from the VPM4 neurons, together with inputs from other as yet unidentified OA neurons. Interestingly, axonal projections of the VPM4 neurons (marked by synaptotagmin fused to GFP; *UASsyt::eGFP*) [32] innervate large areas of the brain, including the PAM cluster, as well as the ventral ganglion (VG), whereas dendritic inputs to VPM4 (*UASDenmark*) [33] are restricted to regions of the central brain and include the SEZ (Figure 2F). Physical proximity of octopaminergic and PAM neurons has also been demonstrated earlier [9, 34].

Extended Flight Bouts Require Oamb on PAM-DANs that Project to MB-β'1

The PAM neuronal cluster projects to various lobes of the MB, a central brain neuropil region. Individual behavioral outputs are dependent upon the activity in specific MB lobes. To understand how dopaminergic PAM outputs influence flight bout durations, strains that mark subsets of PAM neurons and project to different

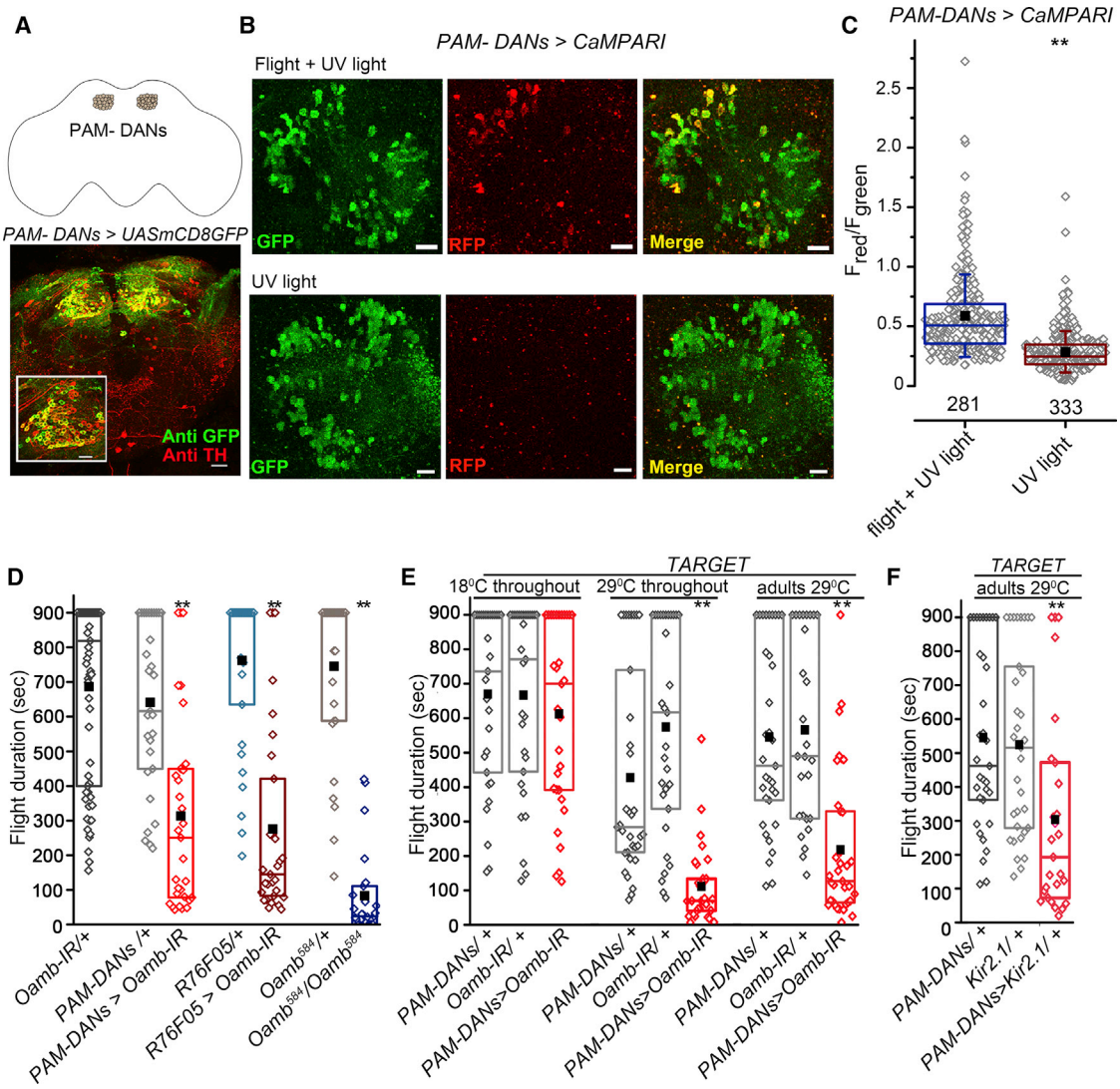

Figure 1. Adult Dopaminergic PAM Neurons Are Active during Flight and Require the Octopamine Receptor Oamb for Sustained Flight

(A) Relative position of the PAM neurons in a fly brain (top). PAM neurons are marked by GFP (*PAM-DANs GAL4>UASmCD8GFP*) and anti-TH antibody (bottom). Scale bar, 10 μm. PAM neurons are shown at a higher magnification in the inset. Scale bar, 5 μm.

(B) Representative images of PAM neurons expressing the neural activity sensor CaMPARI with (top row) or without (bottom row) air-puff-stimulated flight. Conversion of green (GFP) to red (RFP) fluorescence occurs when Ca^{2+} levels increase upon flight-stimulated neural activity and coincide with the presence of UV light, as shown by the red cells (RFP) in the middle panel of the top row. Images are Z projects of selected confocal stacks to visualize the PAM neurons. Scale bars, 10 μm.

(C) Boxplots depicting the ratio of F_{red}/F_{green} values from individual PAM cells ($n \geq 250$; N = 5 brains). The box limit indicates 25th to 75th percentiles; line and square represent median and mean, respectively; whiskers represent SD; and open diamonds represent individual data points. **$p < 0.01$; one-way ANOVA; compared between flight + UV and UV.

(D) Boxplots depicting air-puff-stimulated flight durations of flies with *Oamb* knockdown in PAM neurons, with *PAM-DANs GAL4* (*R58E02-GAL4*), a second PAM-expressing strain *R76F05-GAL4*, and *Oamb*-null mutants. **$p < 0.01$; Mann-Whitney U test was used to compare experimental genotypes with both the heterozygous parental controls; $n \geq 25$. "+" represents a wild-type allele in the parental control genotypes.

(E) Duration of flight bouts in flies with temporal knockdown of *Oamb* in PAM neurons. Stage-specific knockdowns were performed with the TARGET system by temperature shift from 18°C (no knockdown) to 29°C (knockdown) for inactivation of the *GAL80^{ts}* transgene driven by the *tubulin* promoter (*tubGAL80^{ts}*).

(F) Inactivation of PAM neurons by adult expression of a hyperpolarizing potassium channel *Kir2.1* for 5 days reduced the duration of flight bouts. **$p < 0.01$; Mann-Whitney U test was used to compare experimental genotypes with both the parental controls; $n \geq 25$.

See also Figure S1 and Table S1.

lobes of the MB were tested (PAM-MB) [13]. Flight bout durations were measured in organisms with knockdown of *Oamb* in PAM neurons projecting to the β'1, β'2, and γ lobes of MB (Figure 3A). A significant reduction in flight was observed by *Oamb* knockdown in PAM neurons that project to MB-β'1 (*PAM-β'1 GAL4* and *PAM-β'1, β'2, γ GAL4*), whereas *Oamb* knockdown in either

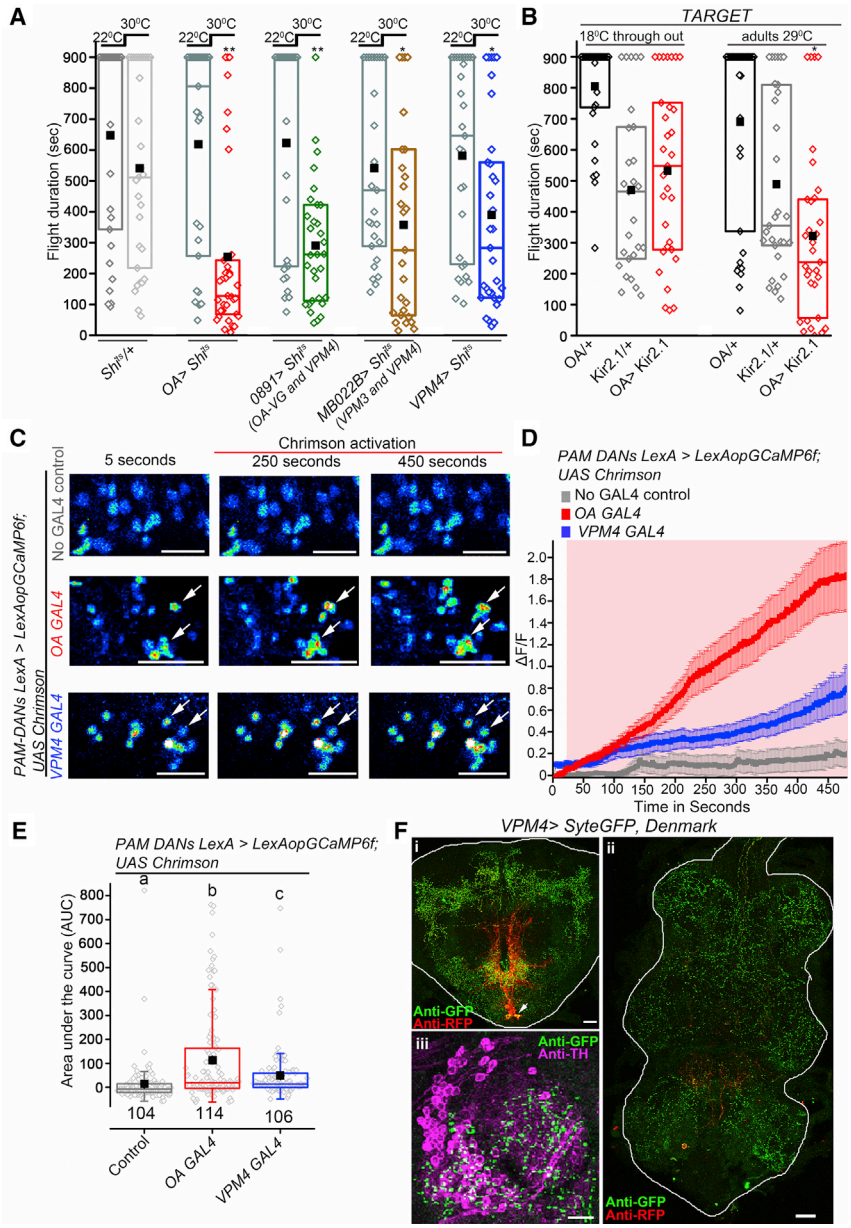

Figure 2. OA Neuron Activity Is Required for Adult Flight and Stimulates the PAM-DANs

(A) Flight deficits observed upon blocking synaptic vesicle recycling by expression of a temperature-sensitive dynamin mutant *Shibire^{ts}* (*Shi^{ts}*) in all octopaminergic neurons (*OA-GAL4* or *Tdc2-GAL4*) and in the indicated subsets of octopaminergic neurons. *0891-GAL4* marks some OA neurons in the SEZ (including VPM4) and in the ventral ganglion (OA-VG). *p < 0.05; **p < 0.01; a Mann-Whitney U test was used to compare the same genotypes 30°C and 22°C; n ≥ 25.

(B) Inactivation of OA neurons by adult expression of a hyperpolarizing potassium channel *Kir2.1* for 5 days reduced the duration of flight bouts. **p < 0.01. For statistics, see Figure 1; n ≥ 25.

(C) Representative images of calcium activity as measured by increase in GCaMP6f fluorescence in PAM neurons of the indicated genotypes. OA neurons were optogenetically activated by red light after 30 s (indicated by a red line). Visible increase in fluorescence was observed in cells marked with white arrowheads by optogenetic activation of OA neurons.

(D) Traces represent time series of normalized GCaMP6f response (mean ± SEM) from PAM neurons (n > 100; N ≥ 5 brains).

(E) Quantification of area under the curve (AUC) from (D). Boxplots and symbols are as described in Figure 1B. Different letters indicate statistically different groups by one-way ANOVA followed by post hoc Tukey's test. $p = 2.4 \times 10^{-6}$ for AUC of control versus *OA-GAL4* and p = 0.011 for AUC of control versus *VPM4 GAL4* (or *MB113C-GAL4*). Numbers below each boxplot indicate the total number of cells imaged.

(F) Confocal images of axonal and dendritic projections of VPM4 neurons by expression of an axonal (SyteGFP) and dendritic (Denmark) marker. (i) Protocerebrum and (ii) ventral ganglion of *VPM4>UAS syt::eGFP*, *UAS Denmark* flies are shown. VPM4 cell bodies are shown by a white arrow. (iii) Axonal projections from VPM4 reach the PAM neurons counterstained with anti-TH (magenta).

Scale bars, 10 μm. See also Table S1.

PAM-β'2 (marked by *PAM-β'2 GAL4*) or γ3 (marked by *PAM-γ3 GAL4*) did not affect flight to a significant extent (Figure 3A). Similarly, knockdown of Oamb in PAM neurons projecting to other remaining MB lobes did not elicit flight deficits (Figure S2A), suggesting that the flight bout deficits arise from PAM projections to the β'1 lobe. This idea was tested further by blocking synaptic vesicle recycling with *Shi^{ts}* in PAM-MBs and testing for flight at a non-permissive temperature of 30°C. Flight deficits were observed upon blocking synaptic vesicle recycling with *Shi^{ts}* in PAM-β'1 and PAM-β'1, β'2, γ, whereas no deficits were observed by inactivation of synaptic vesicle recycling in PAM-β'2 and PAM-γ3 lobes (Figure 3B). However, the defect observed with PAM-β'1 was less severe as compared with PAM-β'1, β'2, γ, possibly due to a difference in the strength of the GAL4 drivers. Taken together, these data suggest that neuronal activity in PAM-MB β'1, β'2, γ modulates flight bout durations, but the requirement for Oamb, in the context of flight, is most likely specific to PAM-β'1. The axonal projections of *PAM-β'1 GAL4* were confirmed as specific to β'1 lobe of MB by expression of a pre-synaptic marker *UASSyt::eGFP*, whereas dendritic projections were visualized with *UASDenmark* (Figure 3C).

To understand whether octopaminergic modulation of PAM-β'1 neurons is specific for flight or whether the effects are more general, we measured other motor functions, such as male courtship behavior and walking activity by two independent assays. Knockdown of *Oamb* in either a majority of PAM neurons (*PAM-DANs>Oamb-IR*) or PAM-β'1 neurons (*PAM-β'1>Oamb-IR*) did not affect the courtship bout number, mean bout duration, and total bout duration to a significant extent (Figures S2B–S2D). Similarly, we did not observe a significant change in walking activity, measured

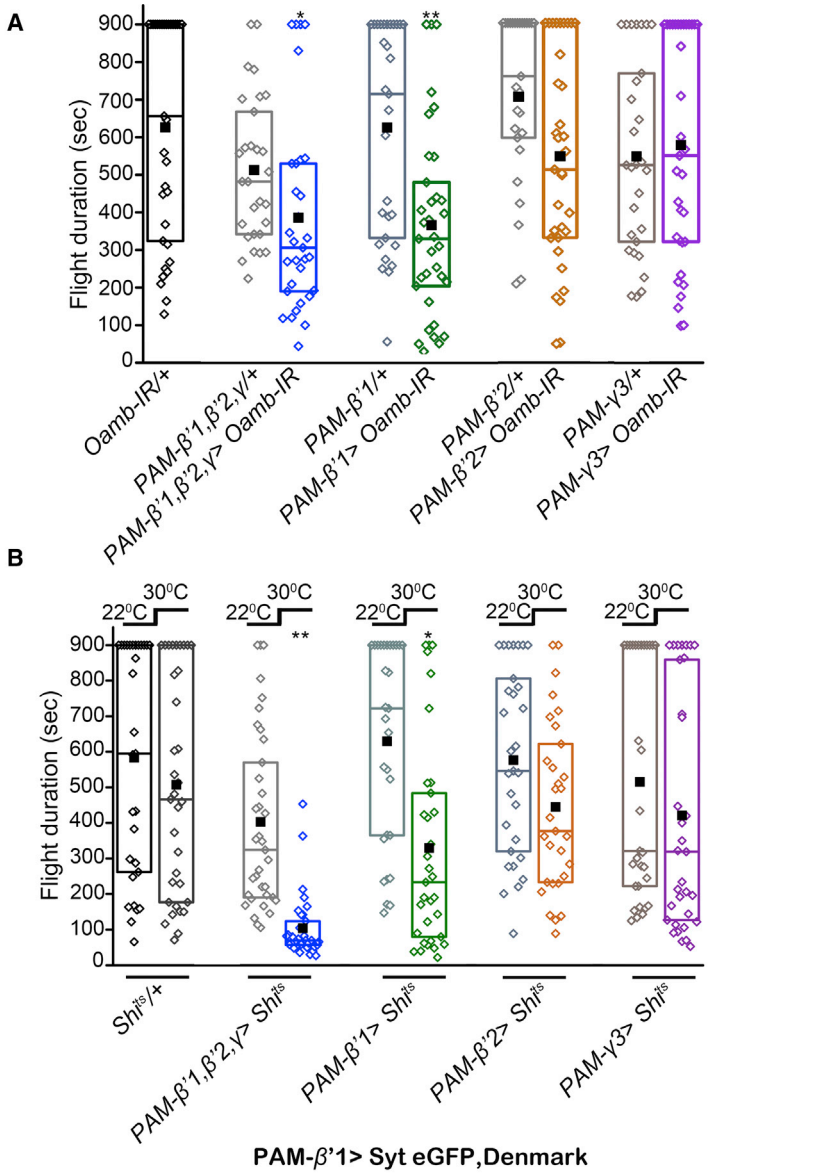

Figure 3. Octopaminergic Inputs for Long Flight Bouts Are Received by PAM-DANs that Project to MB β'1

(A) Flight bout durations observed by knockdown of *Oamb* in the indicated PAM-DAN subsets. For statistics, see Figure 1; n ≥ 25.

(B) Longer flight bouts are reduced significantly by acute inactivation of synaptic vesicle recycling (subset GAL4>*Shi*^{ts} at 30°C) in PAM-β'1 neurons. For statistics, see Figure 2; n ≥ 25.

(C) Confocal images of axonal (left, GFP) and dendritic (middle, RFP) projections of PAM-β'1 neurons (*PAM-β'1>UASSyt::eGFP, UASDenmark*). Axonal projections of PAM-β'1 neurons reach the MB β'1 lobe as shown in the merge panel. Scale bars, 20 μm. *PAM-DAN GAL4* subsets used are described in STAR Methods.

See also Figure S2.

over a total of 45 min, upon knockdown of *Oamb* in either all PAM neurons (*PAM-DANs>Oamb-IR*) or PAM-β'1 neurons (*PAM-β'1> Oamb-IR*; Figures S2E and S2F). Thus, octopaminergic modulation of the PAM-β'1 neurons appear specific for flight and does not affect other motor behaviors requiring either wing or leg movements, such as courtship and walking.

Activation of GABAergic MBON-β'1 Results in Shorter Flight Bouts

The role of MB-β'1 output neurons (MBON-β'1), which are known to be GABAergic [13], was tested next. Flight bout durations decreased significantly upon thermogenetic activation of MBON-β'1 in adults, by expression of *dTrpA1*, a temperature-activated cation channel [35] (Figure 4A) driven by *MB078C-GAL4* (henceforth referred to as *MBON-β'1 GAL4*). Optogenetic activation of MBON-β'1 in adults either with *CsChrimson* [31] or with a mutant white-light-activated channelrhodopsin (*UASChR2XXL*) [36] also decreased the duration of flight bouts (Figures 4B and S3A). Inhibition of MBON-β'1 by expression of *shibire*^{ts} did not alter flight bouts to a significant extent (Figure S3B). These data indicate that, unlike inhibition of either PAM-DANs (Figure 1F) or OA neurons (Figures 2A and 2B), MBON-β'1 inhibition permits extended flight bouts, similar to the controls. Interestingly, when flight bouts were observed for the maximum duration of flight upon optogenetic inhibition of MBON-β'1, by expression of a light-activated chloride pump (halorhodopsin; *eNpHR2*) [37], the median flight time observed (~1,000 s) was similar between control and experimental conditions (Figure S3C). These data suggest that inhibition of the identified MBON-β'1 allows flight bout durations to the same extent as in controls. Activation of PAM-DANs with *CsChrimson* also did not alter the maximum flight durations of control and experimental animals (Figure S3C). For flight bouts that last beyond the maximum time observed in our experimental paradigms, it is likely that MBON-β'1 output is integrated with sensory feedback from other neural circuits. This requires further investigation. Neither activation nor inhibition of another set of MBONs, γ3 (*MBON-γ3 GAL4*), caused any flight deficits (Figures S3A and S3B), suggesting a specific requirement of MBON-β'1 in regulating flight durations.

Thus, activation of β'1 GABAergic ONs reduced flight bout durations, whereas inhibition of activity in the same ONs did not

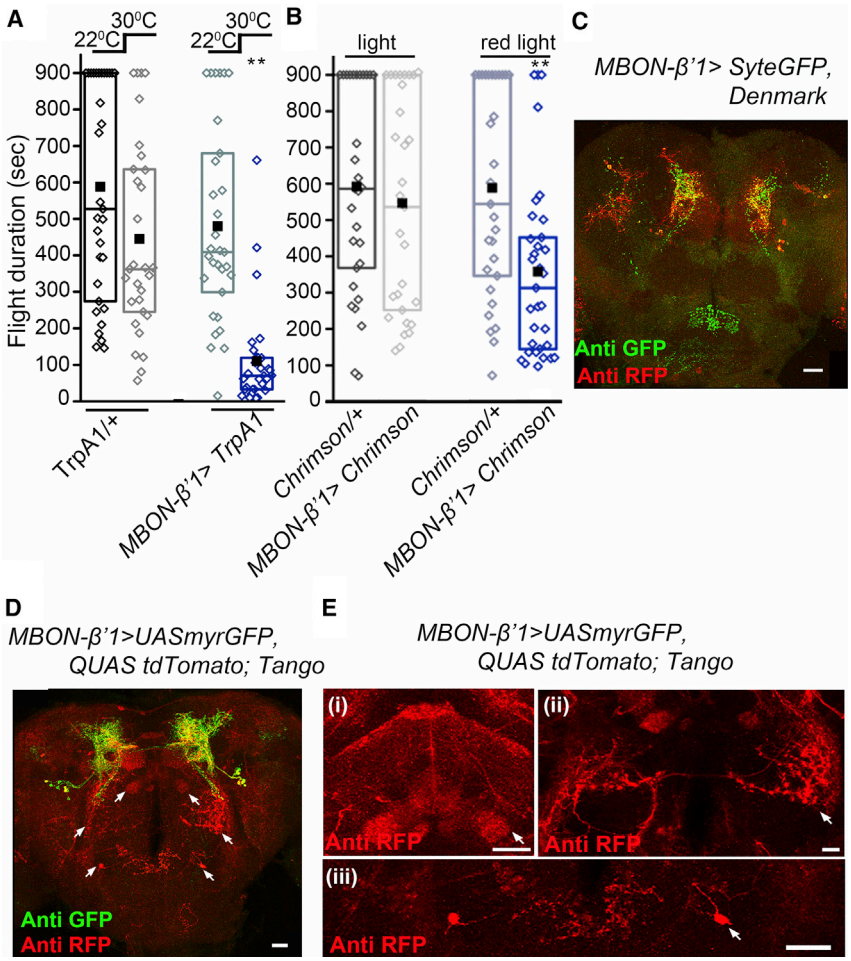

Figure 4. Flight Bout Durations Are Reduced by Activation of GABAergic MBON-β'1 that Projects to the SEZ

(A) Flight bout durations in flies upon thermogenetic activation of MBON-β'1 by expression of *TrpA1*. Boxplots and symbols are as described in Figure 1B. **p < 0.01; Mann-Whitney U test as compared with control *TrpA1*/+ at 30°C and the same genotype at 22°C; n ≥ 25.

(B) Flight bout durations measured upon optogenetic activation of MBON-β'1 by expression of *Chrimson*. Flies for this experiment were reared in the dark until the time of testing, and experimental flies were tested in red light for activation. As controls, flies of the same genotype were tested in white light. **p < 0.01; Mann-Whitney U test as compared with both *Chrimson*/+ tested in red light and the *MBON-β'1>Chrimson* in white light; n ≥ 25.

(C) Representative image of axonal (green) and dendritic projections (red) of MBON-β'1 neurons (*MBON-β'1>UASsyt::eGFP, UASDenmark*).

(D) Confocal image of *trans*-synaptic partners of MBON-β'1 identified by expression of trans-TANGO. Pre-synaptic neurons appear green, and post-synaptic regions appear red. Arrowheads indicate regions of the brain in (E).

(E) Separate confocal stacks of post-synaptic regions of MBON-β'1 as visualized by anti-RFP staining of trans-Tango. (i) Fan-shaped body, (ii) lateral accessory lobe, and (iii) prow region of anterior SEZ are shown.

Scale bars indicate 10 μm. The *MBON-β'1 GAL4* used corresponds to *MB078C-GAL4*. See also Figure S3.

affect flight, suggesting that increasing GABA release from MBON-β'1 by their activation decreases the duration of flight bouts. *Syt::eGFP, Denmark* staining of *MBON-β'1 GAL4* reveals that these MB-ONs project to the SEZ in the protocerebrum of *Drosophila* brain (Figure 4C). Further, we identified *trans*-synaptic partners of MBON- β'1 by the trans-TANGO method [38]. As compared to controls, anti-RFP staining for trans-TANGO was observed in the fan-shaped body of the central complex, the lateral accessory lobe, and prow region of the anterior SEZ (Figures 4D, 4E, S3D, and S3E). These data suggest that GABAergic inhibitory outputs from β'1 modulate sensorimotor outputs from SEZ and parts of the central complex.

Activation of PAM-DANs Reduces Ca^{2+} Transients in the GABAergic MBONs of the β'1 Lobe

Both inhibition of PAM-DANs (Figure 1F) and activation of GABAergic MBON-β'1 (Figures 4A, 4B, and S3A) resulted in reduced flight bout durations. Based on these data, we hypothesized that long flight bouts require OA-stimulated activity in PAM-DANs that in turn inhibits GABAergic MBON-β'1. To test this hypothesis, PAM-DANs were optogenetically activated with red light (*PAM-DANs GAL4>UASChrimson*) and Ca^{2+} transients were monitored in MBON-β'1 (*R30C01-LexA>LexAopGCaMP6f*) from *ex vivo* adult brain explants (Figures 5A and 5B). Upon optogenetic activation of PAM-DANs expressing *CsChrimson*, a significant decrease in the intensity of baseline Ca^{2+} transients were observed in MBON-β'1 as compared to controls (Figures 5C–5E). Thus, activation of PAM-DANs evoked by *CsChrimson* inhibits the activity of MBON-β'1. Taken together, these data support the idea that maintenance of flight bout durations requires OA-stimulated dopamine release for inhibition of activity in GABAergic outputs from MBONs of the β'1 lobe.

Oamb Knockdown in PAM-DANs Affects Free Flight

To assess the relevance of the observed deficits during tethered flight in the context of free flight, we tested flight of *PAM-DANs>Oamb* knockdown flies in a wind tunnel. An appetitive odor (apple cider vinegar) was placed on a high-contrast object at one end of the wind tunnel. Flies starved for 12 hr were released in batches of ten from one end of the wind tunnel, with the air flow from the opposite direction, to ensure that an appetitive odor plume traverses toward the introduced flies (Figure 6A; for details, see STAR Methods). Flies were released at time t = 0 s but were video recorded only from the time they entered the area of capture (AOC) (Figure 6A). Single fly trajectories for two wild-type and two *PAM-DANs>Oamb-IR* knockdown flies are shown in Figure 6B, where the trajectories on the right show flies that landed at the odor source, whereas the trajectories on the left show flies that did not land at the odor source. Additional

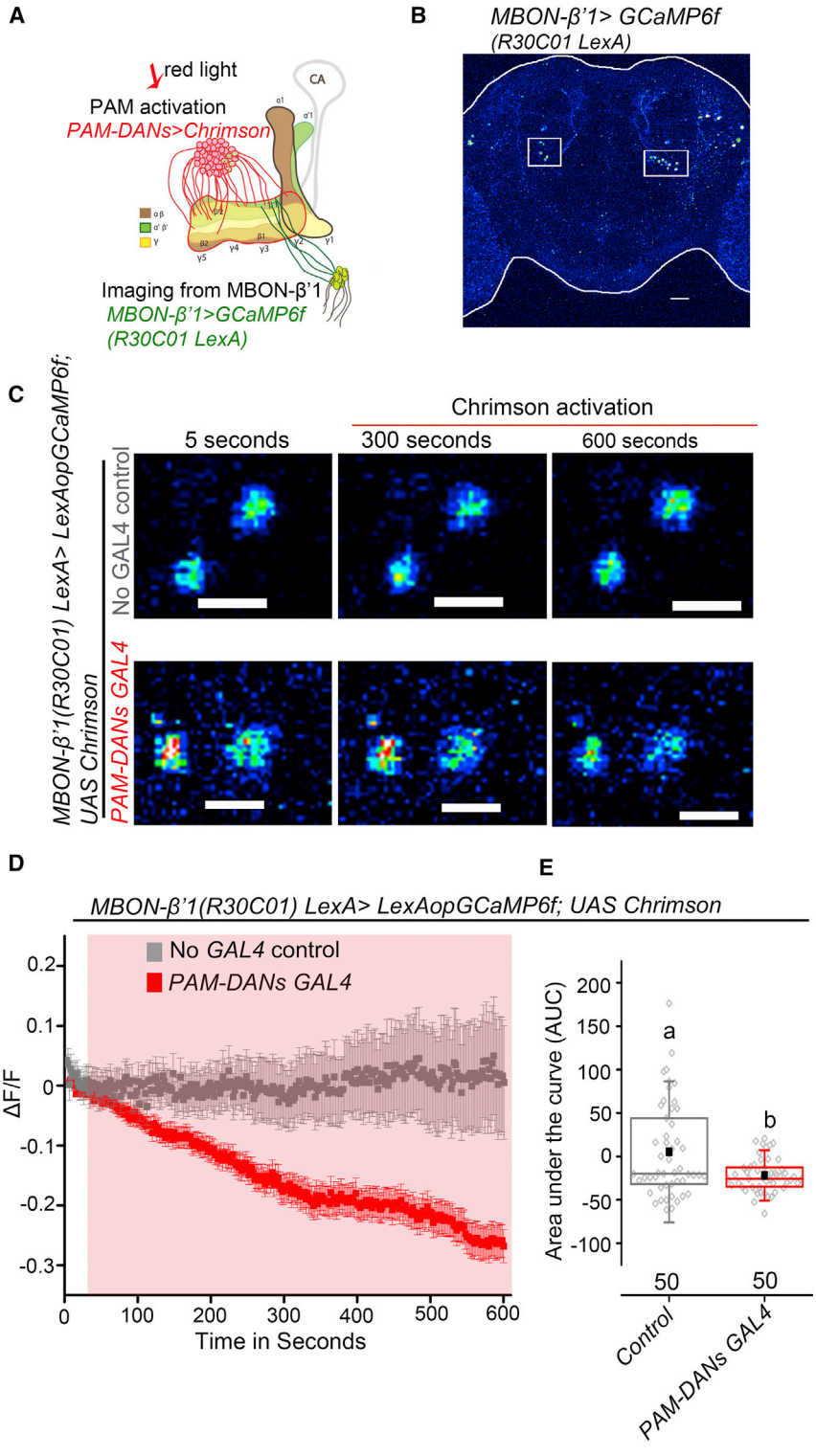

Figure 5. Activation of PAM-DANs Reduces Ca^{2+} Transients in GABAergic MBONs of the β'1 Lobe

(A and B) Cartoon representing (A) simultaneous optogenetic activation of PAM-DANs and imaging of calcium responses from MBON-β'1 marked by (B) *R30C01-LexA>LexAop-GCaMP6f*. Calcium responses were measured from cells within the inset. Scale bar, 10 μm.

(C) Representative images of changes in calcium activity as measured by GCaMP6f fluorescence in MBON-β'1 cells from control (top row) and experimental (bottom row) genotypes evoked upon optogenetic activation of PAM-DANs expressing Chrimson. PAM-DANs were activated with red light (indicated by a red line), and GCaMP6f fluorescence was measured at the indicated time points.

(D) Traces represent time series of normalized GCaMP6f responses (mean ± SEM) from MBON-β'1 of the indicated genotypes upon stimulation with red light.

(E) Quantification of area under the curve from (D). Different letters represent $p < 0.05$ (one-way ANOVA followed by post hoc Tukey's test). Boxplots and symbols are as described in Figure 1B. Numbers below each boxplot indicate the number of cells imaged from at least 5 brains. The *PAM-DANs GAL4* used is *R58E02-GAL4*.

representative single-fly trajectories from a single trial of 10 flies for both wild-type (*CS*) and *PAM-DANs>Oamb-IR* are shown in Figure S4. When flies with knockdown of *Oamb* in the PAM-DANs (*PAM-DANs>Oamb-IR*) were released in the wind tunnel, a significantly smaller number of flies landed at the odor source (Figure 6C). Total flight duration and the number of flight trajectories observed in the AOC were significantly reduced in *Oamb* knockdowns as compared to controls (Figures 6D and 6E), indicating an inability of *PAM-DANs>Oamb-IR* to enter the AOC and fly to the odor source in the wind tunnel. This could potentially be due to their inability to fly for periods of greater than 300 s, as observed in the tethered flight assay (Figure 1C).

Next, we tested the odor-sensing ability of flies with Oamb knockdown in PAM neurons. The response of control and experimental animals to three different odors appeared similar, demonstrating that the reduced number of landings in *PAM-DANs>Oamb-IR* flies is not due to defective odor sensing (Figure S5A). Because cameras in the wind tunnel cover only the last 25 cm of the flight path, initiation of flight is not monitored, and an alternate explanation for fewer flies reaching the odor source is that *PAM-DANs>Oamb-IR* flies fail to initiate flight in the wind tunnel. Therefore, we measured the time taken by *PAM-DANs>Oamb-IR* flies to initiate flight in the absence of an air puff stimulus and compared this with controls. No significant differences between experimental and control genotypes were observed (Figure S5B), indicating that initiation of flight occurs normally in *PAM-DANs>Oamb-IR* flies. We also considered the possibility that *PAM-DANs>Oamb-IR* flies are not motivated to reach the odor source because their metabolic

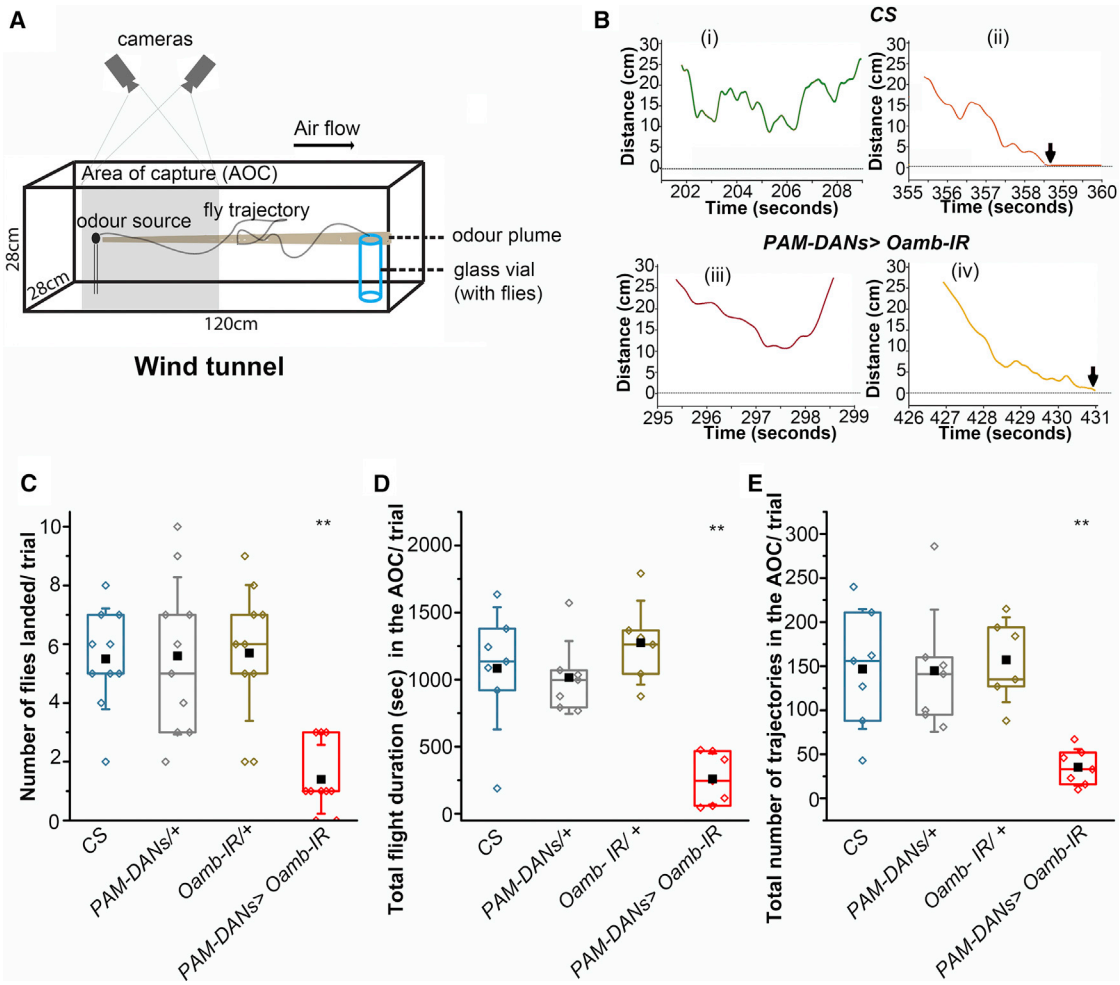

Figure 6. Odor Tracking during Free Flight Is Attenuated in Flies with Oamb Knockdown in the PAM-DANs

(A) Schematic representation of a wind tunnel used for testing the ability of flies to land on an odor source after free flight. Two cameras mounted above the wind tunnel can film flies in real time once they enter in the shaded area. Ten flies are introduced for a single trial, and 10 trials were conducted for each genotype (for details, see STAR Methods).

(B) Representative single-fly trajectories of flies that either landed on the object at distance 0 cm (ii and iv) or flew toward the odor source but did not land (i and iii). Dashed line at 0 cm indicates the odor source, and arrowheads indicate landing. Flies were introduced at time t = 0 s and were video recorded once they enter the area of capture (AOC).

(C) Boxplot with quantification of the number of flies that landed per trial (**$p < 0.01$; Mann-Whitney U test as compared with all three control genotypes).

(D) Boxplot representing the summated flight duration of 10 flies per trial in the AOC (**$p < 0.01$; Mann-Whitney U test).

(E) Boxplot with quantification of the number of flight trajectories obtained in the area captured by the cameras, per trial of 10 flies (**$p < 0.01$; Mann-Whitney U test). Diamonds represent values from individual trials (see STAR Methods). Error bars represent SD in (C)–(E). The *PAM-DANs GAL4* used is *R58E02-GAL4*. See also Figures S4 and S5.

demands are reduced and, therefore, despite the starvation period, they are not hungry. However, in two independent feeding assays, these flies fed normally, suggesting that their metabolic demands upon starvation are no different from controls (Figures S5C and S5D). Thus, Oamb is required in PAM-DANs for normal odor-guided free flight in semi-natural conditions and the absence of octopaminergic inputs to the PAM-DANs results in flies with reduced durations of flight bouts after normal flight initiation.

DISCUSSION

In this study, we describe a neural circuit where octopaminergic inputs, which include neurons in the SEZ, activate a subset of flight-promoting PAM-DANs that project to the MB-β'1 lobe. Output from MB-β'1 lobe is known to be GABAergic [13]. Inhibition of PAM-DAN inputs to the β'1 lobe (Figure 3B) and activation of β'1 GABAergic outputs (Figures 4A, 4B, and S3A) reduce the duration of flight bouts. Moreover, Ca^{2+} imaging experiments demonstrate that activation of the PAM-DANs inhibits activity of GABAergic MBON-β'1 (Figures 5C–5E). It is known that modulation of Kenyon cell and MB-ON synapses by dopamine can alter their synaptic strength over tens of seconds in either positive or negative directions, depending on the context [12]. Our data support a circuit where octopaminergic inputs to PAM-DANs reduce inhibitory GABAergic outputs of MBONs to central brain centers that process visual (FB), gustatory (SEZ), and other

inputs. The identified circuit thus very likely helps integrate multiple sensory cues to sustain longer flight bouts.

Flight Bout Durations Could Be Potentiated by Sensory Feeding Inputs from SEZ-OA to PAM-DANs

Among multiple octopaminergic inputs to PAM-DANs, we have focused on four pairs of SEZ neurons, referred to as the OA-VPM4 (Figure 2A). From marking the axonal (*Syt::eGFP*) and dendritic (*DenMark*) domains of OA-VPM4 neurons, it is clear that they receive inputs primarily from regions near the SEZ, whereas they send information to regions across the brain, including the VG (Figure 2F). The OA-VPM4 neurons have recently been implicated in promoting feeding initiation [39]. In honeybees, electrical stimulation of deep SEZ with high current intensity initiated flight [40]. Although the precise sensory inputs to the OA neurons remain unclear, the SEZ receives proprioceptive information regarding feeding from the head, the mouth cavity, and the trunk [41] as well as mechanosensory inputs from thoracic bristles, eye bristles, wings, and halteres [42]. Moreover, in the SEZ, the adult gnathal ganglion receives inputs from descending neurons that connect to the wing and leg neuropil regions in the ventral nerve cord [43]. Based on these data, we speculate that OA-VPM4 neurons in the SEZ receive a range of sensory information that includes availability of food sources and food intake, and together, such inputs to the OA-VPM4 interneurons help maintain the fly's "flight state" by stimulation of the PAM-DANs.

Long Flight Bouts Require Activity in a Subset of PAM-DANs

Although activity in PAM neurons has previously been implicated in the maintenance of flight [8], we now show that PAM neurons are indeed active during flight (Figures 1A and 1B). Among the ~100 PAM neurons observed per brain hemisphere in *Drosophila*, neural activity was apparent in a subset, suggesting that not all PAM neurons regulate flight. Though selective activation of PAM neurons by flight may be attributed to unequal penetration of UV light through the adult cuticle, this is unlikely, given that, in subsequent experiments, we demonstrate that flight deficits are related to a subset of PAM-DANs (Figure 3A). Knockdown of both the Oamb and Octβ1 receptors in PAM neurons resulted in flight deficits (Figures 1C and S1A), suggesting that OA influences PAM-DAN activity through multiple inputs. The ability of PAM-DANs to permit spatially restricted potentiation or depression of KC-MBON neurotransmission *in vivo* [12] suggests that the identified neural circuit might be active in the natural environment in real time, as, for example, when the fly is unable to find food by walking and therefore needs to fly and integrate appetitive odors with visual cues in search of a food source. Our free flight experiments support this hypothesis (Figure 6).

Activity in PAM-DANs Reduces GABA Release from MBONs to Support Longer Flight Bouts

In addition to olfactory learning and memory [13], MBs modulate satiation-state-dependent foraging [44], mating behavior [45], startle-induced negative geotaxis [46], and flight [6, 8]. In the context of flight, how and which lobes of the MB regulate bout durations has been unclear. In this study, we show that PAM-dopaminergic (DA) inputs to the MB-β'1 lobe inhibit activity of GABAergic ONs (Figure 5). We propose that, in the absence of OA inputs to PAM-DA, the intrinsic baseline activity of GABAergic MBON-β'1 promotes the state of rest and thus prevents longer flight bouts. DA release from OA-stimulated PAMs inhibits the GABAergic β'1 MB-ONs and shifts the fly toward the flight state, allowing for longer flight bout durations (Figures 4A and 5C–5E).

Dopaminergic modulation of flight most likely occurs through dopamine receptors (DopRs) present on either the MB-ONs or the KCs. Both Dop1R1 and Dop1R2 are highly expressed in KC-MB [47, 48]. We have previously shown that knockdown of Dop1R2 in KC-α', β' lobes and inhibition of KC-α', β' using *Shibire^{ts}* resulted in flight deficits, whereas knockdown of Dop1R1 did not [8]. OA-stimulated dopamine release from PAM-β'1 thus very likely activates the KC>MBON-β'1 inhibitory synapses through Dop1R2.

Several recent studies agree with such a circuit. For example, activation of octopaminergic VPM4 neurons decreased GCaMP responses in MBON-γ1pedc>α/β neurons [49] and activation of PAM-DANs decreased Ca^{2+} transients in MBON-γ4 *in vivo* [12]. In addition to MB-β'1, recent data from our group demonstrate neuropeptidergic modulation of other central DANs (PPL1) that project to the vertical MB lobes and also regulate duration of flight bouts [50]. Perhaps, in a fly's natural environment, different classes of sensory stimuli are received by separate DANs, modulating the outputs of distinct MB lobes. Synapses between the Kenyon cells and MB-ONs may thus act as a "switchboard," where multiple sensory signals are interpreted based on the internal state of the fly to drive relevant motor outputs [12].

Modulation of flight behavior by the MB has also been observed in honeybees, where flight orientation is accompanied by transcription of activity-dependent genes in the MB [6]. Another study showed that foraging frequency is associated with MB neuron activity [7], supporting the idea that the MBs integrate food search with flight behavior in honeybees too. In the mammalian context, it may be speculated that MB action is similar to the basal ganglia, which functions like an action selection center based on cues from different sensory parts of the brain [51]. The MBONs could thus be similar to the GABAergic output nuclei of the basal ganglia with a high tonic activity at rest. When explorative locomotion is the action selected by basal ganglia, activity in the GABAergic neurons decreases, which in turn relieves the inhibition of downstream neurons in the mesencephalic locomotor region [52]. During rest, GABA released from the MBONs might inhibit neuronal inputs to downstream neurons, in this case, most likely neurons of the flight central pattern generator that control activity of the flight motoneurons, thus inhibiting flight. When flight needs to be maintained for a longer period, the appropriate sensory stimuli relieve this GABAergic inhibition, resulting in longer durations of flight.

STAR★METHODS

Detailed methods are provided in the online version of this paper and include the following:

- KEY RESOURCES TABLE
- CONTACT FOR REAGENT AND RESOURCE SHARING
- EXPERIMENTAL MODEL AND SUBJECT DETAILS

SUPPLEMENTAL INFORMATION

Supplemental Information includes five figures and one table and can be found with this article online at https://doi.org/10.1016/j.cub.2018.11.070.

A video abstract is available at https://doi.org/10.1016/j.cub.2018.11.070#mmc3.

ACKNOWLEDGMENTS

This study was supported by a grant from CEFIPRA (no. IFC/A/5103-2) to G.H., S.P.S., and J.-F.F. S.B.M. was supported by a fellowship from the National Centre for Biological Sciences, TIFR. We thank Megha, Siddharth Jayakumar and Sufia Sadaf for help with various protocols. We thank the Fly Facility and Central Imaging and Flow Facility at NCBS.

AUTHOR CONTRIBUTIONS

S.B.M. and G.H. designed the study; S.B.M., M.K., and J.-F.F. performed the experiments and analyzed data; and S.B.M. and G.H. wrote the manuscript. J.-F.F., S.P.S., and G.H. critically revised the manuscript.

DECLARATION OF INTERESTS

The authors declare no competing interests.

Received: August 29, 2018
Revised: November 14, 2018
Accepted: November 29, 2018
Published: January 3, 2019

REFERENCES

1. Mamiya, A., and Dickinson, M.H. (2015). Antennal mechanosensory neurons mediate wing motor reflexes in flying *Drosophila*. J. Neurosci. *35*, 7977–7991.
2. Green, J., Adachi, A., Shah, K.K., Hirokawa, J.D., Magani, P.S., and Maimon, G. (2017). A neural circuit architecture for angular integration in *Drosophila*. Nature *546*, 101–106.
3. Buchner, E., Buchner, S., and Bülthoff, I. (1984). Deoxyglucose mapping of nervous activity induced in *Drosophila* brain by visual movement. J. Comp. Physiol. A *155*, 471–483.
4. Weir, P.T., and Dickinson, M.H. (2015). Functional divisions for visual processing in the central brain of flying *Drosophila*. Proc. Natl. Acad. Sci. USA *112*, E5523–E5532.
5. Sane, S.P., Dieudonné, A., Willis, M.A., and Daniel, T.L. (2007). Antennal mechanosensors mediate flight control in moths. Science *315*, 863–866.
6. Lutz, C.C., and Robinson, G.E. (2013). Activity-dependent gene expression in honey bee mushroom bodies in response to orientation flight. J. Exp. Biol. *216*, 2031–2038.
7. Kiya, T., Kunieda, T., and Kubo, T. (2007). Increased neural activity of a mushroom body neuron subtype in the brains of forager honeybees. PLoS ONE *2*, e371.
8. Agrawal, T., and Hasan, G. (2015). Maturation of a central brain flight circuit in *Drosophila* requires Fz2/Ca^{2+} signaling. eLife *4*, e07046.
9. Burke, C.J., Huetteroth, W., Owald, D., Perisse, E., Krashes, M.J., Das, G., Gohl, D., Silies, M., Certel, S., and Waddell, S. (2012). Layered reward signalling through octopamine and dopamine in *Drosophila*. Nature *492*, 433–437.
10. Liu, C., Plaçais, P.-Y., Yamagata, N., Pfeiffer, B.D., Aso, Y., Friedrich, A.B., Siwanowicz, I., Rubin, G.M., Preat, T., and Tanimoto, H. (2012). A subset of dopamine neurons signals reward for odour memory in *Drosophila*. Nature *488*, 512–516.
11. Aso, Y., Herb, A., Ogueta, M., Siwanowicz, I., Templier, T., Friedrich, A.B., Ito, K., Scholz, H., and Tanimoto, H. (2012). Three dopamine pathways induce aversive odor memories with different stability. PLoS Genet. *8*, e1002768.
12. Cohn, R., Morantte, I., and Ruta, V. (2015). Coordinated and compartmentalized neuromodulation shapes sensory processing in *Drosophila*. Cell *163*, 1742–1755.
13. Aso, Y., Hattori, D., Yu, Y., Johnston, R.M., Iyer, N.A., Ngo, T.-T., Dionne, H., Abbott, L.F., Axel, R., Tanimoto, H., and Rubin, G.M. (2014). The neuronal architecture of the mushroom body provides a logic for associative learning. eLife *3*, e04577.
14. Mao, Z., and Davis, R.L. (2009). Eight different types of dopaminergic neurons innervate the *Drosophila* mushroom body neuropil: anatomical and physiological heterogeneity. Front. Neural Circuits *3*, 5.
15. Brembs, B., Christiansen, F., Pflüger, H.J., and Duch, C. (2007). Flight initiation and maintenance deficits in flies with genetically altered biogenic amine levels. J. Neurosci. *27*, 11122–11131.
16. Suver, M.P., Mamiya, A., and Dickinson, M.H. (2012). Octopamine neurons mediate flight-induced modulation of visual processing in *Drosophila*. Curr. Biol. *22*, 2294–2302.
17. Vierk, R., Pflueger, H.J., and Duch, C. (2009). Differential effects of octopamine and tyramine on the central pattern generator for Manduca flight. J. Comp. Physiol. A Neuroethol. Sens. Neural Behav. Physiol. *195*, 265–277.
18. Rillich, J., Stevenson, P.A., and Pflueger, H.-J. (2013). Flight and walking in locusts-cholinergic co-activation, temporal coupling and its modulation by biogenic amines. PLoS ONE *8*, e62899.
19. Huetteroth, W., Perisse, E., Lin, S., Klappenbach, M., Burke, C., and Waddell, S. (2015). Sweet taste and nutrient value subdivide rewarding dopaminergic neurons in *Drosophila*. Curr. Biol. *25*, 751–758.
20. Crocker, A., Shahidullah, M., Levitan, I.B., and Sehgal, A. (2010). Identification of a neural circuit that underlies the effects of octopamine on sleep:wake behavior. Neuron *65*, 670–681.
21. Watanabe, K., Chiu, H., Pfeiffer, B.D., Wong, A.M., Hoopfer, E.D., Rubin, G.M., and Anderson, D.J. (2017). A circuit node that integrates convergent input from neuromodulatory and social behavior-promoting neurons to control aggression in *Drosophila*. Neuron *95*, 1112–1128.e7.
22. Branch, A., Zhang, Y., and Shen, P. (2017). Genetic and neurobiological analyses of the noradrenergic-like system in vulnerability to sugar overconsumption using a *Drosophila* model. Sci. Rep. *7*, 17642.
23. Lee, H.-G., Rohila, S., and Han, K.-A. (2009). The octopamine receptor OAMB mediates ovulation via Ca2+/calmodulin-dependent protein kinase II in the *Drosophila* oviduct epithelium. PLoS ONE *4*, e4716.
24. Fosque, B.F., Sun, Y., Dana, H., Yang, C.T., Ohyama, T., Tadross, M.R., Patel, R., Zlatic, M., Kim, D.S., Ahrens, M.B., et al. (2015). Neural circuits. Labeling of active neural circuits in vivo with designed calcium integrators. Science *347*, 755–760.
25. Lee, H.-G., Seong, C.-S., Kim, Y.-C., Davis, R.L., and Han, K.-A. (2003). Octopamine receptor OAMB is required for ovulation in *Drosophila melanogaster*. Dev. Biol. *264*, 179–190.

26. Xie, T., Ho, M.C.W., Liu, Q., Horiuchi, W., Lin, C.-C., Task, D., Luan, H., White, B.H., Potter, C.J., and Wu, M.N. (2018). A genetic toolkit for dissecting dopamine circuit function in *Drosophila*. Cell Rep. *23*, 652–665.
27. McGuire, S.E., Mao, Z., and Davis, R.L. (2004). Spatiotemporal gene expression targeting with the TARGET and gene-switch systems in *Drosophila*. Sci. STKE *2004*, pl6.
28. Baines, R.A., Uhler, J.P., Thompson, A., Sweeney, S.T., and Bate, M. (2001). Altered electrical properties in *Drosophila* neurons developing without synaptic transmission. J. Neurosci. *21*, 1523–1531.
29. Cole, S.H., Carney, G.E., McClung, C.A., Willard, S.S., Taylor, B.J., and Hirsh, J. (2005). Two functional but noncomplementing *Drosophila* tyrosine decarboxylase genes: distinct roles for neural tyramine and octopamine in female fertility. J. Biol. Chem. *280*, 14948–14955.
30. Kitamoto, T. (2001). Conditional modification of behavior in *Drosophila* by targeted expression of a temperature-sensitive shibire allele in defined neurons. J. Neurobiol. *47*, 81–92.
31. Klapoetke, N.C., Murata, Y., Kim, S.S., Pulver, S.R., Birdsey-Benson, A., Cho, Y.K., Morimoto, T.K., Chuong, A.S., Carpenter, E.J., Tian, Z., et al. (2014). Independent optical excitation of distinct neural populations. Nat. Methods *11*, 338–346.
32. Zhang, Y.Q., Rodesch, C.K., and Broadie, K. (2002). Living synaptic vesicle marker: synaptotagmin-GFP. Genesis *34*, 142–145.
33. Nicolaï, L.J., Ramaekers, A., Raemaekers, T., Drozdzecki, A., Mauss, A.S., Yan, J., Landgraf, M., Annaert, W., and Hassan, B.A. (2010). Genetically encoded dendritic marker sheds light on neuronal connectivity in *Drosophila*. Proc. Natl. Acad. Sci. USA *107*, 20553–20558.
34. Feinberg, E.H., Vanhoven, M.K., Bendesky, A., Wang, G., Fetter, R.D., Shen, K., and Bargmann, C.I. (2008). GFP reconstitution across synaptic partners (GRASP) defines cell contacts and synapses in living nervous systems. Neuron *57*, 353–363.
35. Hamada, F.N., Rosenzweig, M., Kang, K., Pulver, S.R., Ghezzi, A., Jegla, T.J., and Garrity, P.A. (2008). An internal thermal sensor controlling temperature preference in *Drosophila*. Nature *454*, 217–220.
36. Dawydow, A., Gueta, R., Ljaschenko, D., Ullrich, S., Hermann, M., Ehmann, N., Gao, S., Fiala, A., Langenhan, T., Nagel, G., et al. (2014). Channelrhodopsin-2-XXL, a powerful optogenetic tool for low-light applications. Proc. Natl. Acad. Sci. USA *111*, 13972–13977.
37. Berni, J., Pulver, S.R., Griffith, L.C., and Bate, M. (2012). Autonomous circuitry for substrate exploration in freely moving *Drosophila* larvae. Curr. Biol. *22*, 1861–1870.
38. Talay, M., Richman, E.B., Snell, N.J., Hartmann, G.G., Fisher, J.D., Sorkaç, A., Santoyo, J.F., Chou-Freed, C., Nair, N., Johnson, M., et al. (2017). Transsynaptic mapping of second-order taste neurons in flies by trans-Tango. Neuron *96*, 783–795.e4.
39. Youn, H., Kirkhart, C., Chia, J., and Scott, K. (2018). A subset of octopaminergic neurons that promotes feeding initiation in *Drosophila melanogaster*. PLoS ONE *13*, e0198362.
40. Zhao, H., Zheng, N., Ribi, W.A., Zheng, H., Xue, L., Gong, F., Zheng, X., and Hu, F. (2014). Neuromechanism study of insect-machine interface: flight control by neural electrical stimulation. PLoS ONE *9*, e113012.
41. Kendroud, S., Bohra, A.A., Kuert, P.A., Nguyen, B., Guillermin, O., Sprecher, S.G., Reichert, H., VijayRaghavan, K., and Hartenstein, V. (2018). Structure and development of the subesophageal zone of the *Drosophila* brain. II. Sensory compartments. J. Comp. Neurol. *526*, 33–58.
42. Hampel, S., McKellar, C.E., Simpson, J.H., and Seeds, A.M. (2017). Simultaneous activation of parallel sensory pathways promotes a grooming sequence in *Drosophila*. eLife *6*, e28804.
43. Namiki, S., Dickinson, M.H., Wong, A.M., Korff, W., and Card, G.M. (2018). The functional organization of descending sensory-motor pathways in *Drosophila*. eLife *7*, e34272.
44. Landayan, D., Feldman, D.S., and Wolf, F.W. (2018). Satiation state-dependent dopaminergic control of foraging in *Drosophila*. Sci. Rep. *8*, 5777.
45. Rouse, J., Watkinson, K., and Bretman, A. (2018). Flexible memory controls sperm competition responses in male *Drosophila melanogaster*. Proc. Biol. Sci. *285*, 20180619.
46. Sun, J., Xu, A.Q., Giraud, J., Poppinga, H., Riemensperger, T., Fiala, A., and Birman, S. (2018). Neural control of startle-induced locomotion by the mushroom bodies and associated neurons in *Drosophila*. Front. Syst. Neurosci. *12*, 6.
47. Kim, Y.C., Lee, H.G., and Han, K.A. (2007). D1 dopamine receptor dDA1 is required in the mushroom body neurons for aversive and appetitive learning in *Drosophila*. J. Neurosci. *27*, 7640–7647.
48. Qin, H., Cressy, M., Li, W., Coravos, J.S., Izzi, S.A., and Dubnau, J. (2012). Gamma neurons mediate dopaminergic input during aversive olfactory memory formation in *Drosophila*. Curr. Biol. *22*, 608–614.
49. Sayin, S., De Backer, J.-F., Wosniack, M.E., Lewis, L., Siju, K.P., Frisch, L.-M., Schlegel, P., Edmondson-Stait, A., Sharifi, N., Fisher, C.B., et al. (2018). A neural circuit arbitrates between perseverance and withdrawal in hungry *Drosophila*. bioRxiv. https://doi.org/10.1101/259119.
50. Ravi, P., Trivedi, D., and Hasan, G. (2018). FMRFa receptor stimulated Ca2+ signals alter the activity of flight modulating central dopaminergic neurons in *Drosophila melanogaster*. PLoS Genet. *14*, e1007459.
51. Friend, D.M., and Kravitz, A.V. (2014). Working together: basal ganglia pathways in action selection. Trends Neurosci. *37*, 301–303.
52. Stephenson-Jones, M., Yu, K., Ahrens, S., Tucciarone, J.M., van Huijstee, A.N., Mejia, L.A., Penzo, M.A., Tai, L.H., Wilbrecht, L., and Li, B. (2016). A basal ganglia circuit for evaluating action outcomes. Nature *539*, 289–293.
53. Schindelin, J., Arganda-Carreras, I., Frise, E., Kaynig, V., Longair, M., Pietzsch, T., Preibisch, S., Rueden, C., Saalfeld, S., Schmid, B., et al. (2012). Fiji: an open-source platform for biological-image analysis. Nat. Methods *9*, 676–682.
54. Friard, O., and Gamba, M. (2016). BORIS: a free, versatile open-source event-logging software for video/audio coding and live observations. Methods Ecol. Evol. *7*, 1325–1330.
55. Manjila, S.B., and Hasan, G. (2018). Flight and climbing assay for assessing motor functions in *Drosophila*. Bio-protocol *8*, e2742.
56. Makos, M.A., Kim, Y.-C., Han, K.-A., Heien, M.L., and Ewing, A.G. (2009). In vivo electrochemical measurements of exogenously applied dopamine in *Drosophila melanogaster*. Anal. Chem. *81*, 1848–1854.
57. Pathak, T., Agrawal, T., Richhariya, S., Sadaf, S., and Hasan, G. (2015). Store-operated calcium entry through Orai is required for transcriptional maturation of the flight circuit in *Drosophila*. J. Neurosci. *35*, 13784–13799.
58. Balakireva, M., Stocker, R.F., Gendre, N., and Ferveur, J.F. (1998). Voila, a new *Drosophila* courtship variant that affects the nervous system: behavioral, neural, and genetic characterization. J. Neurosci. *18*, 4335–4343.
59. Saxena, N., Natesan, D., and Sane, S.P. (2018). Odor source localization in complex visual environments by fruit flies. J. Exp. Biol. *221*, jeb172023.
60. Fry, S.N., Bichsel, M., Müller, P., and Robert, D. (2000). Tracking of flying insects using pan-tilt cameras. J. Neurosci. Methods *101*, 59–67.
61. Grangeteau, C., Yahou, F., Everaerts, C., Dupont, S., Farine, J.-P., Beney, L., and Ferveur, J.-F. (2018). Yeast quality in juvenile diet affects *Drosophila melanogaster* adult life traits. Sci. Rep. *8*, 13070.
62. Begg, M., and Hogben, L. (1946). Chemoreceptivity of *Drosophila melanogaster*. Proc. R. Soc. Med. *133*, 1–19.
63. Fuyama, Y. (1976). Behavior genetics of olfactory responses in *Drosophila*. I. Olfactometry and strain differences in *Drosophila melanogaster*. Behav. Genet. *6*, 407–420.
64. Ja, W.W., Carvalho, G.B., Mak, E.M., de la Rosa, N.N., Fang, A.Y., Liong, J.C., Brummel, T., and Benzer, S. (2007). Prandiology of *Drosophila* and the CAFE assay. Proc. Natl. Acad. Sci. USA *104*, 8253–8256.
65. Subramanian, M., Metya, S.K., Sadaf, S., Kumar, S., Schwudke, D., and Hasan, G. (2013). Altered lipid homeostasis in *Drosophila* InsP3 receptor mutants leads to obesity and hyperphagia. Dis. Model. Mech. *6*, 734–744.

STAR★METHODS

KEY RESOURCES TABLE

REAGENT or RESOURCE	SOURCE	IDENTIFIER
Antibodies		
Anti-GFP (chick)	Abcam	Cat#13970; RRID: AB_300798
Anti-RFP (rabbit)	Rockland Immunochemicals, Inc.	Cat#600-401-379; RRID: AB_2209751
Anti- TH (mouse)	ImmunoStar	Cat#22941; RRID: AB_572268
Goat anti-Chicken IgY (H+L), Alexa Fluor 488	Thermo Fischer Scientific	Cat#A-11039; RRID: AB_2534096
Goat anti-Rabbit IgG (H+L), Alexa Fluor 568	Thermo Fischer Scientific	Cat# A-11011; RRID: AB_143157
Goat anti-Mouse IgG (H+L), Alexa Fluor 633	Thermo Fischer Scientific	Cat# A-21052; RRID: AB_2535719
Goat anti-Rabbit IgG (H+L), Alexa Fluor 594	Thermo Fischer Scientific	Cat#A-11037; RRID: AB_2534095
Chemicals, Peptides, and Recombinant Proteins		
Low melt Agarose	Invitrogen	Cat#16520-100
All trans retinal	Sigma-Aldrich	Cat#R2500
Apple cider vinegar	Zeta Food Products, Stockholm, Sweden	N/A
Bromophenol blue	Sigma	Cat#B-5525
Chromotrope FB	Sigma	Cat#214515
Experimental Models: Organisms/Strains		
Canton S	Wild type	N/A
R58E02 GAL4 (PAM-DANs GAL4)	Serge Birman	[10]
UAS CaMPARI	BDSC	BDSC_58761
R76F05 GAL4	BDSC	BDSC 41305
UAS Oamb-IR	VDRC	VDRC 2861
$Oamb^{584}$	Scott Waddell	[25]
Tub $GAL80^{ts}$; R58E02 GAL4	This study	N/A
UAS Oamb-IR; Tub $GAL80^{ts}$	This study	N/A
Tub $GAL80^{ts}$	Albert Chiang	NCBS, Bangalore
UAS Kir2.1	BDSC	BDSC_6595
Tub $GAL80^{ts}$; UAS Kir2.1	This study	N/A
UAS Shi^{ts}	T. Kitamoto	[30]
Tdc2 GAL4 (OA-GAL4)	BDSC [29]	BDSC_9313
0891 GAL4	Scott Waddell	[9]
MB022B GAL4	Split Gal4 collection, Janelia	[13]
MB113C GAL4 (VPM4-GAL4)	Split GAL4 collection, Janelia	[13]
R58E02 LexA (PAM-DANs LexA)	[10]	BDSC_52740
LexAopGCaMP6f	BDSC	BDSC_44277
UAS Chrimson	BDSC	BDSC_55136
R58E02 LexA::LexAopGCaMP6f; UAS Chrimson	This Study	N/A
UAS SyteGFP,DenMark	BDSC	BDSC_33065
MB196B GAL4 (PAM-β'1, β'1, γGAL4)	Split GAL4 collection, Janelia	[13]
MB025B GAL4 (PAM-β'1GAL4)	Split GAL4 collection, Janelia	[13]
MB056B GAL4 (PAM-β'2GAL4)	Split GAL4 collection, Janelia	[13]
MB441B GAL4 (PAM-γ3GAL4)	Split GAL4 collection, Janelia	[13]
UAS TrpA1	BDSC	BDSC_26263
MB078C GAL4 (MBON-β'1GAL4)	Split GAL4 collection, Janelia	[13]
UAS eNpHR2	Leslie Griffith	[37]
UAS myrGFP, QUAS TdTomato; Trans -Tango	Michael Rosbash	[38]

(*Continued on next page*)

Continued

REAGENT or RESOURCE	SOURCE	IDENTIFIER
UAS myrGFP, QUAS TdTomato	Michael Rosbash	[38]
UAS mCD8GFP	BDSC	BDSC_5130
R30C01 LexA	BDSC	BDSC_53652
LexAopGCamp6f; UAS Chrimson	This study	N/A
R30C01 LexA; R58E02 GAL4	This study	N/A
UAS Oamb RNAi (3856R-1(III)	NIG	NIG_3856 R-1(III)
UAS Oct β1R RNAi	NIG	NIG_6919 R-2(II)
UAS Oct β1R RNAi	NIG	NIG_6919 R-3(III)
UAS Oct β1R RNAi	VDRC	VDRC_47896
UAS Oct β2R RNAi	VDRC	VDRC_104050
UAS Oct β2R RNAi	VDRC	VDRC_104524
UAS Oct TyrR RNAi	VDRC	VDRC_26876
UAS Oct TyrR RNAi	VDRC	VDRC_26877
UAS Oct β3R RNAi	VDRC	VDRC_9068
UAS Oct β3R RNAi	VDRC	VDRC_101189
R58E02 GAL4::oamb^{584}	This study	N/A
UAS Oamb K3	David J Anderson	[21]
UAS Oamb K3; oamb^{584}	This study	N/A
UAS Chr2XXL	Georg Nagel	[36]
MB110C GAL4(MBON-γ3GAL4)	Split GAL4 collection, Janelia	[13]
Software and Algorithms		
Origin 7.5	MicroCal, Origin Lab, Northampton, MA, USA	N/A
MATLAB	The MathWorks Inc., Natick, NJ	N/A
Fiji	Open access	[53] (RRID:SCR_002285)
Boris	Open access	[54]

CONTACT FOR REAGENT AND RESOURCE SHARING

Further information and requests for resources and reagents should be directed to and will be fulfilled by the Lead Contact, Gaiti Hasan (gaiti@ncbs.res.in).

EXPERIMENTAL MODEL AND SUBJECT DETAILS

Fly strains

Drosophila strains were grown on standard cornmeal media supplemented with yeast at 25°C unless otherwise specified under a 12:12 hr light:dark (10am:10pm) cycle.

The following stocks were kind gifts from various members of the fly community as mentioned. *R58E02 GAL4 (PAM-DANs GAL4)* and *R58E02 LexA (PAM-DANs LexA)* [10] were from Serge Birman (CNRS, ESPCI Paris Tech, France); *UAS Shi^{ts}* [30] was from Toshi Kitamoto (University of Iowa, Iowa City, IA, USA); *UAS Oamb K3* [21] was from David J Anderson (California Institute of Technology, Pasadena, CA); *0891 GAL4* and *Oamb584* [9] were from Scott Waddell (University of Oxford, Oxford); *UAS Chr2XXL* [36] was from Georg Nagel (University Wurzburg); *UAS myrGFP, QUAS TdTomato; Trans -Tango* was from Michael Rosbash (Brandeis University), *UAS eNpHR2* was from Leslie Griffith (Brandeis University). The GAL80^{ts} strain with two inserts of tubP-GAL80^{ts} was generated by Albert Chiang, NCBS, Bangalore, India.

UAS CAMPARI (BL 58761), *UAS Kir2.1* (BL 6595), *Tdc2 GAL4* (*OA GAL4*) (BL 9313), *UAS Chrimson* (BL 55136), *LexAop GCaMP6f* (BL 44277), *UAS SyteGF,DenMark* (BL 33065), *UAS TrpA1* (BL 26263), *R30C01 LexA* (BL 53652), *UAS mCD8GFP* (BL 5130), *R76F05 GAL4* (BL 41305) were obtained from Bloomington stock center (Indiana University).

RNAi strains for *Oamb* (2861) (Figure 1C), *Oct β1R* (47896), *Oct β2R* (104050, 104524), *Oct TyrR* (26876, 26877), *Oct β3R* (9068, 101189) were obtained from Vienna *Drosophila* Stock Center (VDRC, http://www.vdrc.at).

UAS Oamb RNAi (3856 R-1(III)), *UAS Oct β1R RNAi* (6919 R-2(II), 6919 R-3(III)) were obtained from NIG.

Split GAL4 strains *MB113C GAL4* (*VPM4 GAL4*), *MB022B GAL4*, *MB196B GAL4* (*PAM-β'1, β'1, γ GAL4*), *MB025B GAL4* (*PAM-β'1 GAL4*), *MB056B GAL4* (*PAM-β'2 GAL4*), *MB441B GAL4* (*PAM-γ3 GAL4*), *MB213B GAL4* (*PAM-β1, β2 GAL4*), *MB188B GAL4*

(*PAM-β'1, γ3, γ4 GAL4*), *MB316 GAL4* (*PAM- β'2,γ4 GAL4*), *MB312 GAL4* (*PAM-γ4 GAL4*), *MB078C GAL4* (*MBON-β'1 GAL4*), *MB110C GAL4* (*MBON-γ3 GAL4*) were obtained from Janelia split-GAL4 Driver collection [13].

METHOD DETAILS

Single Flight Assay

Flies of either sex were aged for 3-5 days and tested for flight as explained in detail [55]. Briefly, flies were anaesthetized on ice for a short period (~5min) and tethered between their head and thorax using a thin metal wire and nail polish. Upon recovery, a gentle mouth blown air-puff was given and the flight duration was recorded using a stop watch. Flight durations were recorded for a maximum of 15 min (unless otherwise specified) for $\geq$ 25 individual flies in batches of 10 or less. The choice of 15 min is based on observing flight times of wild-type flies till they stop flying voluntarily, for which the median is 650 s. All control genotypes consist of *GAL4* and *UAS* strains crossed to the wild-type strain, *Canton S*. Flight times are plotted as boxplots using Origin software (OriginLab, Northampton, MA). Each box represents 25th to 75th percentile, solid squares represent the mean and the horizontal line in each box represents the median. Individual data points are represented as open diamonds. For *Shi^{ts}* and *TrpA1* experiments, tethered flies were monitored for flight at the temperature mentioned in each figure. For *Kir2.1* experiments, after 2 days of eclosion flies were transferred into an incubator at 29°C for 5 days and then tested. For *Chrimson* and *eNpHR2* experiments, all experimental and control genotypes were reared in the dark in media supplemented with 2mM all-trans Retinal (ATR) and were tested in red light and green light respectively, as shown in the figures.

Calcium imaging with CAMPARI

Tethered flies (*R58E02>CaMPARI*) were exposed to a 405nm laser with light intensity of ~1W/cm ^{2} at the focal plane for a cumulative 300 s. Experimental flies were given an air-puff, to initiate flight, coupled with UV light (405nm), whereas control flies were exposed to UV light in the absence of an air puff. Brains were dissected subsequently and mounted in PBS. Confocal images were acquired as image stacks of appropriate channels (488 nm and 543 nm) on an Olympus FV1000 confocal microscope (Olympus Corporation, Tokyo, Japan) using a 20X objective. Images were combined and visualized as three-dimensional projections using the FV10-ASW 1.3 viewer (Olympus Corporation). For intensity measurements, cells and an appropriate background region were marked using a region of interest (ROI) selection plugin in Fiji. Intensity per cell was calculated, after subtracting the background. Intensity values were calculated for each cell in the GFP channel (F_{green}). The same ROIs were overlaid on images acquired using the 543 nm laser to calculate cell intensities in the red channel (F_{red}). The intensity was calculated as the ration of F_{red} to F_{green} for each brain sample irrespective of the treatment. Ratios of F_{red} to F_{green} are depicted as boxplots for both air puff stimulated fliers and static controls (OriginLab, Northampton, MA). Each box represents 25th to 75th percentile, solid squares represent the mean and the horizontal line in each box represents the median. Individual cells are represented as open diamonds. A minimum of 5 flies were tested for experimental and control genotypes.

Ex-vivo imaging of adult brains

Adult brains were dissected in adult hemolymph like (AHL) saline [56] and embedded in ~10ul of low melt agarose (Invitrogen) with anterior facing the coverslip. Brains were bathed in 100 μL of AHL. Images were acquired as a time series on an XY plane at an interval of 2sec using a 20X objective on an Olympus FV1000 inverted confocal microscope (Olympus Corp., Japan). For optogenetic stimulation of *Chrimson*, a 633nm laser line was used, while simultaneously acquiring GCaMP6f fluorescence images with a 488nm laser line to measure changes in Ca^{2+}. At least 5 independent brain preparations were used for all live imaging experiments and the exact number of cells imaged are indicated in the figures.

Raw fluorescence data were extracted from the marked ROIs using a time series analyzer plugin in Fiji. ΔF/F was calculated using the following formula for each time point (t): $\Delta F/F = (F_t - F_0)/F_0$, where F_0 is the average basal fluorescence of the first 10 frames. Area under the curve were calculated in Microsoft Excel and values are depicted as boxplots (OriginLab, Northampton, MA).

Immunohistochemistry

Immunostaining was performed on dissected adult CNS (3-4 days old unless otherwise specified) as previously described [57]. Briefly, adult brains with ventral ganglia were dissected in cold 1x PBS and samples were fixed in 4% paraformaldehyde in 1x PBS for 40 min at 4°C. They were washed 3-4 times with 0.3% Triton-X in 1x PBS (PTX) and blocked in blocking solution (5% Normal goat serum in PTX) for 2 hr at room temperature. Following overnight incubation with the appropriate primary antibodies at 4°C, 3-4 washes were performed in PTX and the samples were incubated in appropriate secondary antibodies for 2 hr at room temperature. Primary antibodies were used at the following dilutions: chick anti-GFP (1:8000, #13970, Abcam), mouse anti-TH (1:50, #22941, ImmunoStar), rabbit anti-RFP (1:500, #600-401-379, Rockland). Secondary antibodies were all used at a dilution of 1:400 as follows: anti-chick Alexa Fluor 488 (# A-11039, Thermo Fischer Scientific), anti-rabbit Alexa Fluor 568 (# A-11011, Thermo Fischer Scientific), anti-mouse Alexa Fluor 633 (# A-21052, Thermo Fischer Scientific), anti-rabbit Alexa Fluor 594 (#A11037, Thermo Fischer Scientific). Confocal images were acquired with either a 40X or a 60X objective on a FV1000 or a FV3000 confocal microscope and visualized using a FV10-ASW 4.0 viewer (Olympus) or Fiji.

Courtship assay

Tests were performed with 40 pairs of flies. Each pair consisted of an intact male and a decapitated female. All the flies tested were 5-7 days old and were reared in an incubator with 12 hr dark:light cycle from 8am to 8pm. Assays were performed between 10am - 11.30am on 5 consecutive days. Each single male was aspirated without anesthesia into the observation chamber of 1.6cm^3 and was allowed to acclimatize for 10 min before the female was introduced. Observations were made for a duration of 300sec for each pair. Courtship videos were obtianed using a video camera coupled with a MacIntosh MacBook Air computer and were analyzed using the open Boris software. Bout number, mean bout duration and total bout duration were plotted using Origin software (OriginLab, Northampton, MA) (Figures S2B–S2D).

Locomotor assay

Locomotor assays were performed between 10am - 11.30am as described previously [58]. Briefly, locomotor activity of singly housed males (3-4 days old) was monitored in a circular chamber of diameter of ~4cm. Each fly was introduced into a chamber and allowed to acclimatize for 5 min. A pattern of lines was drawn under the assay chamber and the total number of times lines were crossed by each fly, was monitored for a duration of 10 s. For each experiment, four single flies were sequentially observed for five periods of 10sec, every 2min. The entire experiment was repeated after a duration of 45 min with the same set of flies in the same chamber in order to check for the effect of fatigue, because the flies tested were starved for the entire duration of experiment that lasted for 45 min. Total locomotor activity or Locomotor Activity Units were plotted as the sum of total number of lines crossed by each fly over a duration of 50 s, monitored in bins of 10 s. LAU_{45min} represents the results obtained in the experiment performed with the same flies after 45 min. Locomotor activity at 0 min (LAU_{0min}) and the ratio of locomotor activity of 45 min to 0 min (LAU_{45min} / LAU_{0min}) were plotted using Origin software (OriginLab, Northampton, MA) (Figures S2E and S2F). A minimum of 20 flies were tested for each genotype.

Free flight tracking in a wind tunnel

Experiments were performed with 3-5 days old flies during the light cycle (10am to 11.30am) in order to coincide with the flies' photoperiod. The flies were starved overnight in a damp chamber for 12 hr prior to the experiment in order to increase their motivation to forage.

The chamber of the custom-made wind tunnel used is 28cm x 28cm x 120cm [59]. Part of the wind tunnel was calibrated for imaging flies using two cameras that overlooked the wind tunnel and a predefined scale. The sides and base of the working section in the wind tunnel were covered with white sheets of paper to enhance contrast with respect to the background. Wind tunnel illumination for tracking the flies are as described in [59]. The average illumination within the chamber was ~350 lux, as measured by a light meter (Center 337 light meter).

During the experiment, a 10 μL drop of apple cider vinegar was placed on a black bead and used as the odor source. The black bead was glued to a transparent glass capillary (10cm tall and 1mm thick) placed within a small Plexiglas holder. This odor source was introduced in the wind tunnel with a low speed laminar air flow of 0.1 m/s. After the odor source was placed in the chamber and the wind turbines started, ten flies of a particular genotype were released simultaneously from one end that was opposite to the odor source and the timer was started. Flight trajectories were filmed with two Basler cameras (acA640-120 gm GigE) at 120 frames per second for 10 min and processed by Trackit 3-D [60] software, and the time taken for each fly to land was noted. After 10 min the recording was stopped and all the flies were flushed out of the wind tunnel. The same flies were never used for repeated experiments. The raw 3D co-ordinates were processed and fly trajectories were plotted using custom written MATLAB (License number 1122786; host ID: A4BADB34D85C) codes. These codes are available on request. Boxplots and bar graphs for landing were plotted in Origin software (OriginLab, Northampton, MA)

Odor sensitivity assay

5-day old males were individually maintained in a fresh food vial since adult emergence. 16 hr before the test, each male was kept in an empty glass vial containing only a humid filter paper (ø = 19 mm with 0.6 mL pure water). Tests were always performed between 9am and 1pm. After a brief anesthesia on ice, individual males were individually introduced into the straight arm of a Y-shape olfactometer made by a small glass vial. This arm is connected via the dividing arms of the olfactometer to an empty glass vial, each one containing a small filter paper (ø = 11mm) impregnated with the tested substance. In the case of plain food, filter papers were incubated overnight at 25°C in fresh food vials [61]. For the other substances (acetic acid, ethyl acetate, pure water), small filter papers were added with 50 μL just before the test. Acetic acid and ethyl acetate were diluted in distilled water at 2.5% and 0.1%, respectively, according to previous studies [62, 63]. The test was performed over a 120-min period under far-red light (LED bulbs). After the test start, the position of the fly in the device was noted every 10min relative to the arm chosen. Flies from all genotypes were simultaneously tested, and each substance was tested over several days. Significant differences between genotypes were determined with a Fisher's exact test.

Flight initiation assay

Flight initiation by 3-4 days old male flies was monitored in a transparent plexiglass chamber of dimensions 25cm × 25cm × 25cm. A single male fly was allowed to climb a thin transparent tube (3.5cm height and 3mm diameter) kept vertically at the bottom of the chamber. Once the fly reached the tip of the tube the time taken to initiate flight was measured for a maximum of 10 min. The

experiment was repeated with a minimum of 30 flies per genotype to be tested. Initiation data were plotted using Origin software (OriginLab, Northampton, MA).

CAFE assay

The CAFÉ assay was performed as described previously with minor modifications [64]. Culture plates with 24 wells (#351147, Corning) and with small holes at the bottom of each well for aeration were lined with a thin layer of wet filter paper cut to the diameter of the well to ensure sufficient humidity. Calibrated glass micropipettes (5 μL, #P0549, Sigma) were filled with 0.5 μL of liquid food, consisting of Sucrose 0.27 g, yeast extract 0.18 g and 300 μL of 0.5% bromophenol blue in 4.7 mL of double distilled water, by capillary action. To monitor food intake a 4 days old single male fly was introduced into one well and a capillary with food was suspended into each well. Capillary tubes with food were replaced with fresh tubes every day. The volume of food consumed per day per fly was measured for 4 days consecutively. Data for the first day were excluded when calculating the average consumption of food per fly per day. Data were plotted as bar graphs using Origin software (OriginLab, Northampton, MA). Each bar represents mean of the data points and the error bars represent SEM.

Dye feeding assay

Dye feeding assay was performed as previously described [65]. Briefly, freshly eclosed male flies were collected and aged for 3 days. They were starved for 24 hr and then transferred into vials with media containing 1.2% red dye (Chromotrope FB, Sigma), 1% agar and 100mM sucrose. After 2 hr of feeding inside a dark chamber, intake of red dye was monitored from the abdominal lysates of flies (n = 3) of 3 independent batches.

QUANTIFICATION AND STATISTICAL ANALYSIS

All bar graphs and line plots show means and standard error of means. In boxplots, horizontal lines in the box indicate median, box limits are from 25^{th}- 75^{th} percentiles and individual data points are represented by open diamonds (unless otherwise specified in the figure legends). All statistical tests were performed using Origin 8.0 software, the details of which are explained in individual figure legends.